Available online at www.sciencedirect.com
SCIENCE DIRECT®
PERGAMON
Electrochimica Acta 48 (2003) 2761–2766
ELECTROCHIMICA Acta
www.elsevier.com/locate/electacta

Electronic transport in $Ce_{0.8}Sm_{0.2}O_{1.9-\delta}$ ceramics under reducing conditions

J.C.C. Abrantes [a], D. Pérez-Coll [b], P. Núñez [b], J.R. Frade [c,*]

[a] ESTG, Instituto Politécnico de Viana do Castelo, 4900 Viana do Castelo, Portugal
[b] Department Química Inorgánica, Universidad de La Laguna, E-38200 La Laguna, Tenerife, Spain
[c] Department Engenharia Cerâmica e do Vidro, CICECO, Universidade de Aveiro, 3810-193 Aveiro, Portugal

Received 20 January 2003; received in revised form 6 May 2003; accepted 15 May 2003

Abstract

$Ce_{0.8}Sm_{0.2}O_{1.9-\delta}$ powders were prepared by a freeze drying method and used to obtain ceramic disks. These samples were used to study the electronic transport properties of this material. A Hebb–Wagner method was used to obtain the electronic conductivity under ion blocking conditions. Typical values of electronic conductivity measured for this material at 800 °C were about 0.37 S m^{-1} at $Po_2 = 10^{-16}$ atm and 0.58 S m^{-1} at $P_{O_2} = 10^{-18}$ atm. These values are significantly lower than results reported for ceria-based materials with different trivalent additives. A coulometric titration method was used to estimate the charge carrier concentrations, and the mobility of carriers was obtained on combining the results of conductivity and concentration. Typical values of mobility show weak temperature dependence and decrease with increasing oxygen deficiency, suggesting a limiting value of about 0.5×10^{-7} m^2. V^{-1} s^{-1} for relatively high δ.

Keywords: Ceria–samaria; Electronic conductivity; Oxygen nonstoichiometry; Polaron mobility

1. Introduction

Ceria based materials have attracted great interest as potential electrolyte materials for intermediate temperature solid oxide fuel cells [1–5], with higher ionic conductivity than the standard yttria stabilised zirconia electrolyte. One of the main limitations of ceria based electrolytes is the onset of electronic conductivity under reducing conditions. Yet, this disadvantage of potential electrolyte materials is an advantage for alternative potential applications as components of SOFC anodes [6–10]. This shows the importance of an accurate characterisation of the electronic conductivity of ceria based materials both in order to establish the limits of the electrolytic domains, and/or to optimise the mixed conducting properties for prospective anode materials.

The ionic conductivity of ceria based materials is promoted by suitable trivalent additives such as Gd^{3+}, Sm^{3+} or Y^{3+}. Some authors reported the highest values of ionic conductivity for ceria–gadolinia [5], and this has also been supported by computer atomistic modelling [11]. These simulations predicted a combination of coulombic interactions and lattice relaxation, which vary with the size of the trivalent additive. The lowest overall interaction was predicted for Gd^{3+}. However, the values of trapping energy are also dependent on the fraction of the trivalent additive [4,12]. The ionic conductivity goes through a maximum at intermediate contents of the additive. Other authors [1,2] thus reported higher ionic conductivity values for ceria–samaria materials. Materials with mixed dopants (e.g. $Ce_{1-x-y}Sm_xY_yO_{2-(x+y)/2-\delta}$) may also be promising [13].

Some discrepancies between different authors can also be related to differences in sample preparation, and the corresponding effects on the relative role of resistive grain boundaries, especially at relatively low or intermediate temperatures [14–17]. One may thus expect some improvements by optimizing the powder and ceramic preparation methods.

* Corresponding author. Tel.: +351-370-254; fax: +351-2344-25300.
E-mail address: jfrade@cv.ua.pt (J.R. Frade).

0013-4686/03/$ - see front matter © 2003 Elsevier Ltd. All rights reserved.
doi:10.1016/S0013-4686(03)00395-5

A proper assessment of ceria-based materials for electrochemical applications must also take into account the onset of electronic contributions; this is important to assess the applicability of ceria-based electrolytes, for cases with sufficiently wide electrolytic domain, and/or the applicability as a mixed conducting component of alternative fuel electrodes (e.g. ceria/Ni cermets [6]). The ionic transport number in air is close to unit [1,4], but most ceria-based materials show significant n-type electronic conductivity under typical fuel conditions. Some results suggest that $Ce_{1-x}Sm_xO_{2-x/2-\delta}$ may be less reducible that other ceria-based materials, thus extending the electrolytic domain to more reducing conditions [1]. However, other authors obtained similar results for the dependence of oxygen nonstoichiometry of $Ce_{1-x}Sm_xO_{2-x/2-\delta}$ and $Ce_{1-x}Gd_xO_{2-x/2-\delta}$ on the oxygen partial pressure. It is thus important to re-examine the transport properties of these materials and to resort to different experimental techniques to reassess the main trends. The main techniques used in the present work were an ion blocking technique to measure the electronic conductivity, and a coulometric titration method to evaluate the oxygen nonstoichiometry.

There is a relatively wide consensus that ceria-based materials are mixed conductors [4], due to a combination of transport of oxygen vacancies and small polaron electronic transpor under reducing conditions. The electron hole transport number tends to be low ($t_p < 0.01$) even under oxidising conditions [18,19]. The relative role of the electronic contribution is thus mainly related to the reaction of reduction:

$$O_O^x \rightleftarrows V_O^{\bullet\bullet} + 2e^- + 1/2O_2 \quad (1)$$

and one may use the corresponding mass action constant to describe the dependence of the electronic charge carrier concentration on the oxygen partial pressure:

$$[V_O^{\bullet\bullet}]n^2(P_{O_2})^{1/2} = K_R = \exp(\Delta S_R/R)\exp[-\Delta H_R/RT) \quad (2)$$

The defect chemistry of ceria based electrolytes or mixed conductors is also dependent on suitable aliovalent additives such as Gd^{3+}, Sm^{3+} or Y^{3+}. These additives tend to enhance the concentration of oxygen ion vacancies, and thus the ionic conductivity, as predicted by the overall neutrality condition. For ceria–samaria solid solutions, and on neglecting the contribution of electron holes:

$$2[V_O^{\bullet\bullet}] \approx n + [Sm'_{Ce}] \quad (3)$$

In addition, electron transport in ceria based materials is believed to occur via small polarons, and one may thus consider that the charge carrier corresponds to trivalent cerium ions:

$$n = [Ce'_{Ce}] \quad (4)$$

Note that the concentration of oxygen vacancies $[V_O^{\bullet\bullet}] \approx [Ce'_{Ce}] + [Sm'_{Ce}]$, and thus the oxygen non-stoichiometry depend on the concentrations of both trivalent species, whether dopant or reduced cerium.

For conditions corresponding to the ionic domain of these materials the defect chemistry is still determined by the additive, because the change in oxygen stoichiometry (δ) in $Ce_{1-x}Sm_xO_{2-x/2-\delta}$ remains much smaller than the fraction of the trivalent additive $\delta \ll x$. In this case,

$$[V_O^{\bullet\bullet}] \approx [Sm'_{Ce}]/2 = (x/2)(4/v_o) \quad (5)$$

where v_o is the unit cell volume of the fluorite-type phase. Using formulae proposed to account for the effects of the mol% and ionic radius of the trivalent cation [4] one expects about 1.6×10^{-28} m^3 for $Ce_{0.8}Sm_{0.2}O_{1.9-\delta}$.

The concentration of electrons (or polarons) is related to the change in oxygen stoichiometry:

$$n \approx [Ce'_{Ce}] \approx 2\delta(4/v_o) \quad (6)$$

as indicated by Eqs. (1) and (4). On inserting the expressions obtained for the concentrations of vacancies and electrons in the mass action constant (Eq. (2)) on thus obtains:

$$\delta = [K_R/(2x)]^{1/2}(v_o/4)^{3/2}(P_{O_2})^{-1/4} \quad (7)$$

This condition probably fails for relatively large values of oxygen deficiency, in which case one must re-write:

$$[V_O^{\bullet\bullet}] = (4/v_o)(\delta + x/2) \quad (8)$$

and substitution in Eq. (2) yields the following generic solution:

$$4\delta^2(\delta + x/2)(P_{O_2})^{1/2} = K_R(v_o/4)^3 \quad (9)$$

For relatively low fractions of the trivalent additive and/or large changes in oxygen stoichiometry ($\delta \gg x$), Eq. (9) also yields an alternative power law which is frequently assumed:

$$\delta = (K_R/4)^{1/3}(v_o/4)(P_{O_2})^{-1/6} \quad (10)$$

Eq. (9) suggest a representation of $4\delta^2(\delta + x/2)(P_{O_2})^{1/2}$ versus δ (or vs. $\log(P_{O_2})$) to obtain the relevant mass action constant, independently of any assumption concerning the limiting cases when the dependence of oxygen nonstoichiometry on oxygen partial pressure might be described by power laws $(P_{O_2})^{-1/4}$ (Eq. (7)) or $(P_{O_2})^{-1/6}$ (Eq. (10)). The enthalpy and entropy of reaction (1) are easily obtained from the temperature dependence of K_R. In addition, Eq. (9) is suitable to detect possible deviations from ideal defect chemistry models derived on assuming diluted media. For example, defect interactions (e.g. association of oxygen vacancies with trivalent cations) are likely to occur in these materials. Experimental errors may also be re-

sponsible for deviations from the expected ideal behaviour.

A combination of Eqs. (6) and (7) indicates the concentration of charge carriers varies as $(P_{O_2})^{-1/4}$, at least for relatively small changes in oxygen stoichiometry. One can thus assume a similar dependence of the electronic conductivity on oxygen partial pressure:

$$\sigma_n \propto (P_{O_2})^{-1/4} \tag{11}$$

except possibly for a slight dependence of the mobility of polaron hopping on oxygen stoichiometry $\mu_h \propto (1-x-2\delta)$. Many authors thus assume the predicted power law (Eq. (11)) or [20]:

$$\sigma = \sigma_I + \sigma_h^* (P_{O_2})^{-1/4} + \sigma_p^* (P_{O_2})^{1/4} \tag{12}$$

which includes the conductivity contributions of oxygen vacancies and electron holes.

Eq. (12) is the basis for the widely used method of extracting the electronic conductivity contributions from the dependence of $\log(\sigma)$ versus $\log(P_{O_2})$ [1,5]. However, the actual results of total conductivity often fail to show the ideal trend, mainly for very reducing conditions when the changes of oxygen stoichiometry cause deviations from a simple power law. The mobility of polarons may also vary significantly with the oxygen stoichiometry due to changes in the corresponding activation energy. In addition, the ionic conductivity can also go through a maximum in the range of strongly reducing conditions, as pointed out by Mogensen et al. [4]. All these effects may contribute to significant deviations from the power law $\sigma \propto (P_{O_2})^{-1/4}$. An alternative ion blocking method was thus used in the present work.

2. Experimental methods

Powder of composition $Ce_{0.8}Sm_{0.2}O_{1.9}$ was prepared by a freeze-drying method, starting from $Ce(NO_3)_3 \cdot 6H_2O$ and $Sm(NO_3)_3 \cdot 6H_2O$ (Aldrich, 99.9%). These nitrates were dissolved in distilled water, and this solution was taken into a separating funnel and dropped into liquid nitrogen, with continuous stirring. The resulting ice crystals were dehydrated in a freeze drier (lyolab 3000, Heto) for 3 days. Additional details of the methods were presented elsewhere [21]. The as prepared powder was amorphous, as found by X-ray diffraction. The freeze-dried powder became crystalline on calcining at 600 °C or higher temperatures. Powder pre-calcined at 1200 °C and then milled again was used to prepare ceramic pellets by uniaxial pressing and sintering at 1600 °C for 10 h. The final density was about 92% of the theoretical density (7.15 g cm^{-3}), evaluated from the unit cell volume of the fluorite-type structure of CSO. These samples were found gas tight.

A coulometric titration cell (Fig. 1) was used to measure the dependence of oxygen stoichiometry on the oxygen partial pressure. This cell comprises separate electrodes for pumping oxygen from inside the cell, and to measure the resulting emf V_o, which was used to obtain the oxygen partial pressure inside the cell (P_{O_2}), as given by the Nernst equation:

$$V_o = [RT/(4F)] \ln[P_{ref}/P_{O_2}] \tag{13}$$

The outside atmosphere was air, thus establishing a reference condition $P_{ref} = 0.21$ atm.

The coulometric titration experiments were performance under increasing applied voltage, with 50 mV steps, and then allowing for steady state conditions to be re-established. The corresponding change in oxygen stoichiometry after a generic step ($\Delta\delta$) was then calculated by integrating the current as follows:

$$\Delta\delta = M_{CSO}(2Fm)^{-1} \int (I - I_\infty)\, dt \tag{14}$$

where M_{CSO} is the formula weight of $Ce_{0.8}Sm_{0.2}O_{1.9}$, m is the mass of the sample, F is the Faraday constant and I_∞ is the residual current. The oxygen stoichiometric changes are very small for a relatively wide range of values of P_{O_2}, starting from zero applied voltage. One thus assumed a reference condition $\delta \approx 0$ for $P_{O_2} = 0.21$ atm.

The n-type conductivity was measured under ion blocking conditions using a Hebb–Wagner method, represented in Fig. 2, and described elsewhere [20]. Other authors [22] obtained blocking conditions by encapsulating a Pt micro-contact pressed against the sample. However, the accuracy of such approach is somewhat dependent on difficulties in obtaining a precise value for the small contact area. Our cell is thus based on larger Pt electrodes, painted on both surfaces of an impervious disk of the CSO. An impervious alumina disk was then pressed against one of those electrodes, and a glass ceramic seal was used to ensure gas tightness and an ion blocking electrode. The experiments were performed with increasing applied

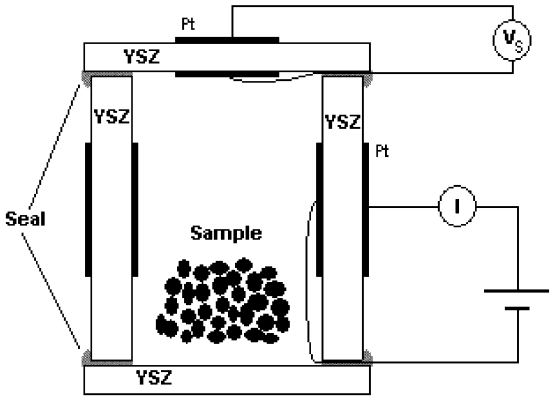

Fig. 1. Schematic representation of the coulometric titration cell.

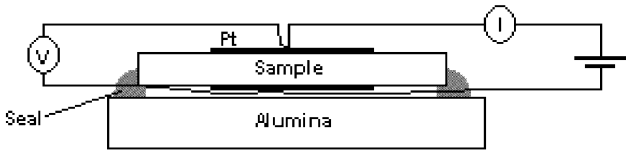

Fig. 2. Schematic representation of the ion blocking method used to measure the electronic conductivity.

voltage, using one pair of Pt wires for the applied voltage and different Pt wires for reading the value of V_o; this value was used to calculate the corresponding value of P_{O_2} (Eq. (13)).

3. Results and discussion

3.1. Changes in oxygen stoichiometry

The dependence of oxygen stoichiometry on the oxygen partial pressure is shown in Fig. 3. Some results extracted from the literature [25] are shown for comparison. The nearly exponential dependence clearly shows significant bending for very reducing conditions. Similar deviations have been reported by other authors [23,24,26], and may indicate either a deviation from a simple defect chemistry model for ideal dilute conditions, or failure of the experimental method. The deviations are confirmed by the alternative representation in Fig. 4, which can be used without any a-priori assumption concerning a limiting power law. Note that Eq. (9) corresponds to the plateau region in Fig. 4, and should account for both regimes (Eq. (7) or Eq. (10)), under ideal or sufficiently dilute conditions. The plateau values $K_R(v_o/4)^3$ are thus useful to extract the mass action constant of the reduction reaction, even for cases showing a transition between different power laws $P_{O_2}{}^{-1/n}$, while avoiding excessive deviations from dilute conditions.

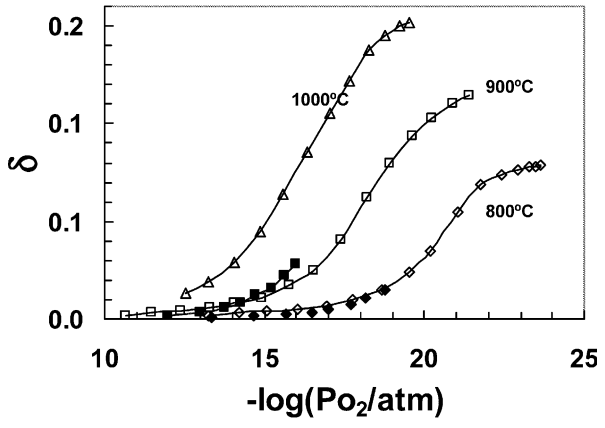

Fig. 3. Dependence of oxygen nonstoichiometry on oxygen partial pressure determined from coulometric titration results. Results extracted from Ref. [25] (closed symbols) are shown for comparison.

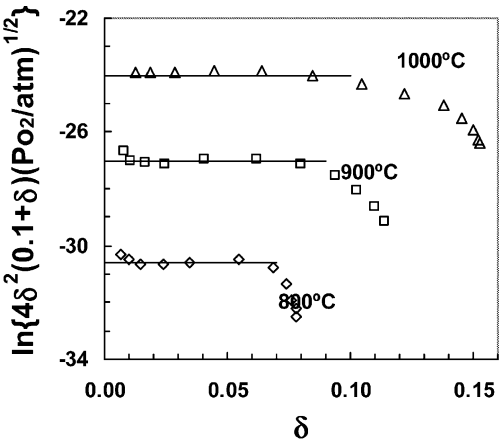

Fig. 4. Alternative representation of the coulometric titration results used to extract the values of mass action constant of the reaction of reduction.

Some authors attributed deviations from an ideal defect chemistry model to association of oxygen vacancies with trivalent cations, including Ce^{3+}, especially for relatively large stoichiometric changes [25]. However those authors were still unable to find a close agreement between the proposed model and experimental results. Atomistic computer simulations confirmed the interactions between oxygen vacancies and trivalent cations [11], and suggested stronger interactions with Ce^{3+} than with other trivalent cations (e.g. Gd^{3+} or Sm^{3+}). Thus, one expects stronger defect interactions for relatively high concentrations of Ce^{3+}, (large δ), and restricted our analysis to a range of relatively small values of δ, within the plateau region in Fig. 4. It is also known that defect association is more likely to occur below a given critical temperature, as revealed by the temperature dependence of conductivity [27,28]. Our results were thus restricted to a temperature range which is clearly above the critical temperature expected for ceria–samaria materials (in the range 600–700 °C [28]).

The values of K_R were thus extracted from the plateau region in Fig. 4, and were used to obtain the corresponding values of enthalpy ΔH and entropy ΔS:

$$\ln(K_R) = -\Delta H/(RT) + \Delta S/R \quad (15)$$

as shown in Fig. 5; this yielded:

$$K_R = 1.43\times10^{90}\ \exp(-45.1\times10^3/T)m^{-9}\ \text{atm}^{1/2} \quad (16)$$

with typical values of enthalpy, $\Delta H = 375$ kJ mol^{-1}, similar to results obtained by other authors for ceria-based materials [25] and yielding the expected range of values of oxygen deficiency.

3.2. n-Type conductivity

Fig. 6 shows the ion blocking results obtained at different temperatures. The electronic current density (J_e) was obtained under steady state ion-blocking

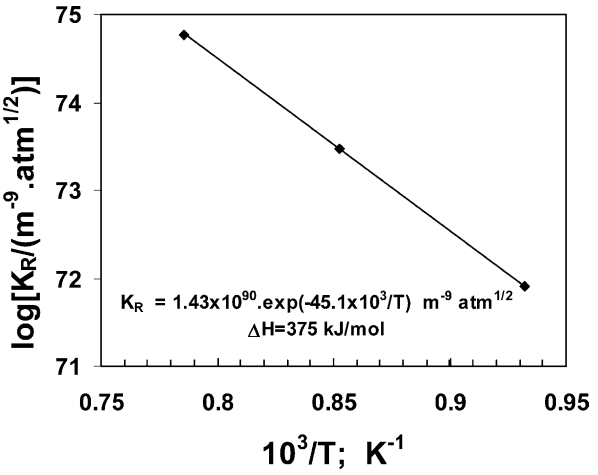

Fig. 5. Temperature dependence of the mass action constant of reduction, used to evaluate the corresponding enthalpy and entropy.

conditions, and can be used to obtain the electronic conductivity [20,22,29]. A generic analytical solution has been proposed to interpret results obtained with Hebb–Wagner techniques on assuming that the total electronic conductivity is $\sigma_e = \sigma_n^*(P_{O_2})^{-1/4} + \sigma_p^*(P_{O_2})^{1/4}$. In this case [22,29]:

$$J_e = (RT/FL) \times \{\sigma_n^*[\exp(V_o F/RT) - 1] + \sigma_p^*[1 - \exp(-V_o F/RT)]\} \quad (17)$$

where L is the thickness of the sample and F is the Faraday constant. However, this solution should not be extended for very reducing conditions, when the $(P_{O_2})^{-1/4}$ power law fails. One should thus retain the differential equation, as proposed by some authors [22]:

$$\sigma_e(V_o) = L\, dJ_e/dV_o \quad (18)$$

In this case, the electronic conductivity is obtained by differentiating the current density against V_o. The corresponding dependence of the electronic conductivity

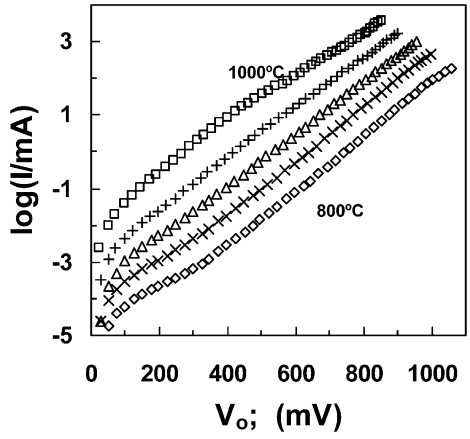

Fig. 6. Ion blocking results obtained for CSO at 800 °C (◇), 850 °C (×), 900 °C (△), 950 °C (+), and 1000 °C (□).

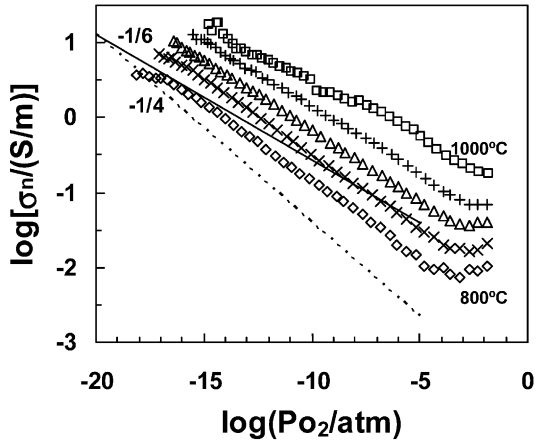

Fig. 7. Electronic conductivity results obtained by differentiating the ion blocking results at 800 °C (◇), 850 °C (×), 900 °C (△), 950 °C (+), and 1000 °C (□).

σ_e on P_{O_2} (Fig. 7) was also obtained by taking into account Eq. (13).

Data treatment is thus achieved without imposing pre-assumptions on the type of dependence of n-type and/or p-type contributions on oxygen partial pressure. Note that the log–log plots of the dependence of electronic conductivity on oxygen partial pressure (Fig. 7) suggest that the actual n-type results deviate from the theoretical −1/4 power law. The results at the highest temperatures (about 1000 °C) are closer to the −1/6 power law, and results obtained at lower temperatures (about 800 °C) indicate intermediate slopes (ca. −1/5). Some results also suggest the onset of the p-type contribution under oxidising conditions.

The polaron mobility was also estimated on combining the results of electronic conductivity and carrier concentrations, extracted from the dependence of oxygen nonstoichiometry on oxygen partial pressure (Fig.

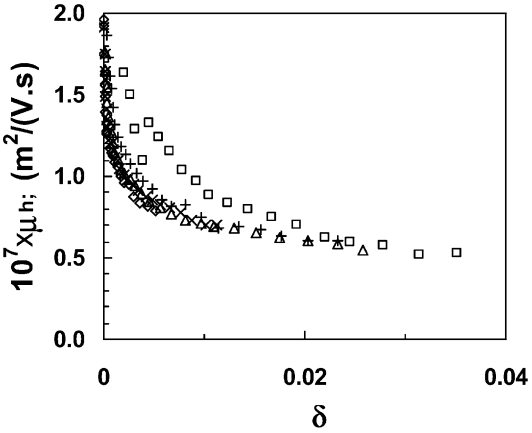

Fig. 8. Dependence of polaron mobility on oxygen nonstoichiometry estimated on combining the dependence of electronic conductivity on the oxygen partial pressure, and the mass action constant of the reaction of reduction (Fig. 5). 800 °C (◇), 850 °C (×), 900 °C (△), 950 °C (+), and 1000 °C (□).

8). Actually, one resorted to the temperature dependence of the equilibrium constant shown in Fig. 5, and used this to obtain the dependence of δ (Eq. (9)) and $[Ce'_{Ce}]$ (Eq. (6)) on P_{O_2}, at different temperatures.

The values of mobility shown in Fig. 8 are significantly lower than reported for undoped ceria, with similar oxygen nonstoichiometry [29]. This may be an advantage of ceria-samaria electrolytes, by contributing to extend the electrolytic domain to more reducing conditions. The present results confirm that the mobility of polarons decreases with increasing oxygen deficiency probably due to defect interactions. Literature data [1,3] indicated that ceria–yttria or ceria–gadolinia materials may be more suitable to increase the electronic conductivity relative to ceria–samaria. However, it has not been clear whether this corresponds to differences in reducibility or differences in mobility of polarons, and one should thus extend this work to ceria-based materials with different trivalent additives (e.g. Gd, Y, etc.). This understanding will contribute to optimise ceria-based materials for prospective applications requiring mixed conductivity (e.g. anode materials for SOFCs).

4. Conclusions

The electronic transport properties of ceria-samaria materials were studied by a combination of coulometric titration and ion-blocking methods. These results were interpreted without imposing any assumption concerning limiting power laws for the dependence of oxygen stoichiometry and/or electronic conductivity on oxygen partial pressure. The methods used in this work are thus suitable to re-examine relevant transport properties of ceria-based materials under reducing conditions. The results of mobility obtained for ceria–samaria are clearly lower than reported for undoped ceria with similar oxygen nonstoichiometry. This may affect prospective applications requiring mixed conductivity (e.g. anode materials for SOFCs). On the contrary, lower polaron mobility may contribute to extend the electrolytic domain of ceria–samaria electrolytes, relative to materials with other trivalent additives.

Acknowledgements

The authors acknowledge the financial support by a Spanish Research Program (MCYT MAT2001-3334) and by the Portuguese Foundation for Science and Technology (FCT). Travel grants were provided by the European Science Foundation (OSSEP Programme) for bilateral cooperation. One of the authors (D.P.C.) was supported by a Cajacanarias-ULL Program

References

[1] H. Yahiro, K. Eguchi, H. Arai, Solid State Ionics 36 (1989) 71.
[2] K. Eguchi, T. Setoguchi, T. Inoue, H. Arai, Solid State Ionics 52 (1992) 165.
[3] H. Inaba, H. Tagawa, Solid State Ionics 83 (1996) 1.
[4] M. Mogensen, N.M. Sammes, G.A. Tompsett, Solid State Ionics 129 (2000) 63.
[5] B.C.H. Steele, Solid State Ionics 129 (2000) 95.
[6] M. Mogensen, T. Lindegaard, U.R. Hansen, G. Mogensen, J. Electrochem. Soc. 141 (1994) 2122.
[7] S. Park, J.M. Vohs, R.J. Gorte, Nature 404 (2000) 265.
[8] E.S. Putna, J. Stubenrauch, J.M. Vohs, R.J. Gorte, Langmuir 11 (1995) 4832.
[9] Y. Okawa, T. Matsumoto, T. Doi, Y. Hirata, J. Mater. Res. 17 (2002) 2266.
[10] S. Wang, T. Kato, S. Nagata, T. Honda, T. Kaneko, N. Iwashita, M. Dokiya, J. Electrochem. Soc. 149 (2002) A927.
[11] L. Minervini, M.O. Zacata, R.W. Grimes, Solid State Ionics 116 (1999) 339.
[12] G.B. Jung, T.J. Huang, C.L. Chang, J. Solid State Electrochem. 6 (2002) 225.
[13] J. van Herle, D. Seneviratne, A.J. McEvoy, J. Eur. Ceram. Soc. 19 (1999) 843.
[14] K. El Adham, A. Hammou, Solid State Ionics 9 (1983) 905.
[15] G.M. Christie, F.P.F. van Berkel, Solid State Ionics 83 (1996) 17.
[16] J. van Herle, T. Horita, T. Kawada, N. Sakai, H. Yokokawa, M. Dokiya, J. Eur. Ceram. Soc. 16 (1996) 961.
[17] I. Riess, D. Braunshtein, D.S. Tannhauser, J. Am. Ceram. Soc. 64 (1981) 479.
[18] F.M. Figueiredo, F.M.B. Marques, J.R. Frade, J. Eur. Ceram. Soc. 19 (1999) 639.
[19] D.P. Fagg, J.C.C. Abrantes, D. Pérez-Coll, P. Núñez, V.V. Kharton, J.R. Frade, Electrochim. Acta 48 (2003) 1023.
[20] L. Navarro, F. Marques, J. Frade, J. Electrochem. Soc. 144 (1997) 267.
[21] D. Pérez-Coll, P. Núñez, J.R. Frade, J.C.C. Abrantes, Electrochim. Acta 48 (2003) 1551.
[22] S. Lubke, H.D. Wiemhofer, Solid State Ionics 117 (1999) 229.
[23] I. Riess, H. Janczikowski, J. Nolting, J. Appl. Phys. 61 (1987) 4931.
[24] M.A. Panhans, R.N. Blumenthal, Solid State Ionics 60 (1993) 279.
[25] D. Schneider, M. Godickemeier, L.J. Gauckler, J. Electroceramics 1 (1997) 165.
[26] S. Wang, H. Inaba, H. Tagawa, M. Dokiya, T. Hashimoto, Solid State Ionics 107 (1998) 73.
[27] K. Huang, M. Feng, J.B. Goodenough, J. Am. Ceram. Soc. 81 (1998) 357.
[28] G.B. Jung, T.J. Huang, C.L. Chang, J. Solid State Electrochem. 6 (2002) 225.
[29] H.L. Tuller, A.S. Nowick, J. Phys. Chem. Solids 38 (1977) 859.